Efficient Design for PMSM Control and Real-Time Diagnosis based on FreeRTOS for e-bike application

M. Loussif
Laboratoire des Systèmes Electriques,LR11ES
Ecole Nationale d'Ingénieurs de Tunis,
Université Tunis El manar
Department of research and innovation
ACTIA Engineering Services
Tunis, Tunisia
mariem.loussif@etudiant-enit.utm.tn

M.Ayari
Laboratoire des Systèmes Electriques,LR11ES
Ecole Nationale d'Ingénieurs de Tunis,
Université Tunis El manar
Tunis, Tunisia
maissa.ayari@etudiant-enit.utm.tn

L. Charaabi
Laboratoire des Systèmes Electriques,LR11ES
Ecole Nationale d'Ingénieurs de Tunis,
Université Tunis El manar
Tunis, Tunisia
lotfi.charaabi@enit.utm.tn

S.Khojet El Khil
Laboratoire des Systèmes Electriques,LR11ES
Ecole Nationale d'Ingénieurs de Tunis,
Université Tunis El manar
Tunis, Tunisia
sejirkek@gmail.com

S. Sayahi
Department of research and innovation
ACTIA Engineering Services
Technopôle El Ghazala - 1, BP99 rue Newton
Ariana 2088, Tunisia
sofiane.sayahi@actia-engineering.tn

2023 14th International Renewable Energy Congress (IREC) | 979-8-3503-4284-0/23/$31.00 ©2023 IEEE | DOI: 10.1109/IREC59750.2023.10389371

***Abstract*—This paper deals with the freeRTOS-based permanent magnets synchronous motor (PMSM) control algorithm developed by ST microelectronics and the optimal diagnostic tasks implementation in a freeRTOS-based e-bike control firmware. The purpose of this work is to investigate the STM32 freeRTOS-based firmware, to develop and implement optimally the diagnostic tasks of an e-bike PMSM. The implementation of the diagnostic tasks is achieved after a detailed and insightful analysis of the STM32 PMSM control firmware and realized through the utilization of a feature provided via freeRTOS which is: task notification and deferred interrupt handling.**

***Index Terms*—freeRTOS; motor control firmware; FOC; Task notification; deferred interrupt handling; Diagnostic tasks; SOGI; HALL sensors; Power; RMS.**

I. Introduction

The increasing adoption of e-bikes, driven by their eco-friendly nature and cost-effectiveness, intensifies the focus on enhancing the control and performance of electric propulsion systems.

In this paper, we have used a power assist E-bike known also as Pedelec system. This is the most commonly used type of electric bike. It operates as a human-electric hybrid bicycle, providing assistance when the rider starts pedaling. This method generates an assisted torque proportional to the pedaling torque exerted by the rider [10] [12]. The proportional-assist power is often based on velocity [11]. The velocity value must adhere to a specific threshold, typically set at 25 km/h, in accordance with European norms. This threshold represents the maximum allowable speed for the high velocity category. The resulting value will be expressed as a power ratio, which will then be multiplied by the rider's power. Since the E-bikes have limited speed of rotation and require a high torque, PMSs represent the best solution for this type of use case thanks to their, advantages of high power density, high efficiency, light weight, small inertia and small volume [1]. The Field-Oriented Control (FOC) is the main technique used to control the PMSMs. Since, it has established itself as a go-to method for controlling electric motor drives when high torque quality is demanded [1].

A significant advancement discussed in reference [5]is the development of a motor control driver specifically designed for the FreeRtos real-time operating system, based on STM32. This research emphasizes the advantages of using FreeRTOS over conventional software implementations. Notable benefits include optimal utilization of CPU resources and a simplified software architecture design, enhancing the overall performance of motor control systems Like many industrial manufacturers, ST microelectronics has developed a PMSM control firmware that integrates real-time operating systems (RTOS) that is FreeRTOS [5,6]. In the context of e-bike systems, the ability to diagnose is paramount. Thus, we implemented a freeRTOS-based diagnosis tasks that encompasses tasks such as Hall sensor diagnostics, power calculations, the SOGI task and the RMS task. And this diagnostic facet ensures the safety and reliability of the e-bike.

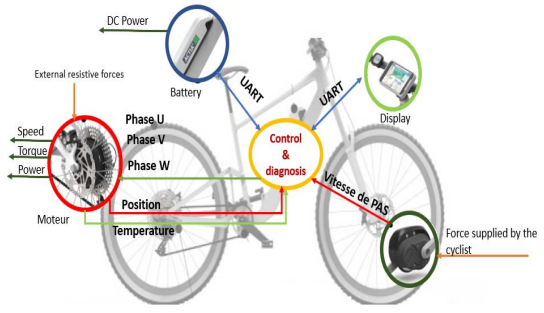

Fig. 1. The e-bike control and diagnosis signals overview

This paper embarks on an exploration of these intertwined elements : the FOC control method, the STM32 PMSM control FreeRTOS-based firmware, and the indispensable diagnosis

axis. By delving into these crucial aspects, we aim to provide a comprehensive understanding of the intricate interplay between technology, control, and diagnostics within the evolving landscape of electric micro-mobility. voltage sensor and Speed controller. The main contribution of this paper is the new method proposed for the implementation of diagnostic tasks, as well as the nature of these diagnostic tasks. This paper is structured as follows. In section, I, the field-oriented control technique is described. Then, section II details the freeRTOS-based firmware PMSM control. Finally, in section III the freeRTOS-based diagnosis tasks implementation is presented with a detailed insight into each diagnostic task of the four tasks and in the section IV,the experimental setup used to validate the freeRTOS-based firmware is presented.

II. Describing the field-oriented control technique:Architecture, Principles, and Performance Analysis

A. Overview of permanent magnets synchronous motor PMSM

From the 1970s onwards, there has been a shift towards using alternating current (AC) machines instead of direct current (DC) machines. Although DC machines offer easy control through flux and torque decoupling, their power and maximum speed are limited due to the presence of brushes, and they require expensive maintenance. In contrast, synchronous electric machines are known for their rotor rotation speed matching the rotating field produced by the stator under a specific load condition. A PSM has two main parts. A fixed, stationary, called stator and another rotating rotor. It is an electromagnetic system based on the principle of rotating the magnetic field of the stator synchronously with the rotor during its operation.

Stator: The stator presents the armature, consisting of a laminated steel with notches where the windings are housed. The latter are grouped in a coil forming three circuits represented by the winding axes (abc) and offset each other by a 120° angle connected most often in a star. The role of armature is to create a rotating magnetic field when it is powered by a three-phase source [9].

Rotor: The rotor, the rotating part of the machine, represents the inductor. It is composed of a laminated ferromagnetic core on which permanent magnets are arranged thus generating a permanent excitation. The number of poles depends on the use of the motor because there is a compromise between torque and speed that must be respected. In other words, the increase in the number of poles will guarantee a better torque on the one hand but a decrease in the maximum speed of rotation on the other hand.

B. Field Oriented control for PMS motors

The field-oriented control (FOC) technique uses linear controllers and pulse-width modulation to control the fundamental components of the load voltages vectors [2], enables a decoupled control of torque and magnetization and a better dynamic performance of the PMSM as it employs mathematical transformations to separate the torque generation and magnetization functions in PMSM.

The basic structure of this control structure is presented in Fig 2.

It consists of the Clarke, Park and inverse Park transformations,3 PI controllers respectively for the Q axis current,D axis current and the speed and the space vector pulse width modulation block.

The Field Oriented Control (FOC) involves the regulation of the stator currents represented by a vector. This control method employs projections to convert a time and speed-dependent three-phase system into a time-invariant system with two coordinates, namely the d and q coordinates.

These projections enable a control structure resembling that of a DC machine.

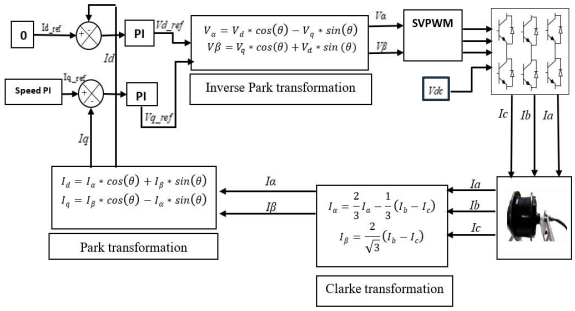

Fig. 2. Block diagram of the FOC technique

III. Analyzing the STM32 freeRTOS PMSM control firmware: tasks structure, prioritization, and functional insights

Awhile back, the FOC was implemented based on single tasks system. This solution limited the performances of the system and the implementation of additional code and module.For this reason, using FeeRTOS as a preemptive and multitask system will increase the efficiency of the motor control by optimizing the use of the Hardware resources including memory and CPU thanks to it management and scheduler capability. It also provides more flexibility to add an independent task that can be executed for certain conditions, which is our case in the diagnosis solution. The used STM32 FreeRTOS-based motor control firmware consists of two tasks[3] where the first is called a medium frequency task and the second is a safety task.

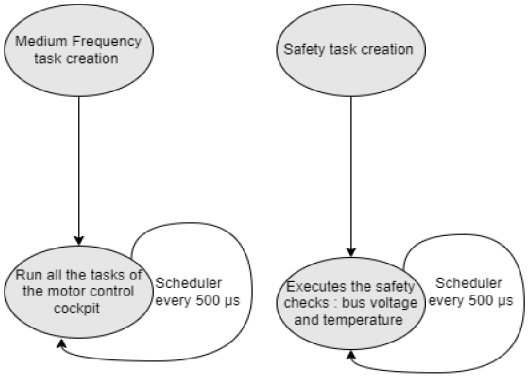

Fig. 3. The MF task and safety task routine flows

A. The medium Frequency task

This task, created with an above-normal priority, runs all the functions of the Motor Control cockpit. In particular, it executes the duties requiring a periodic execution at a medium frequency rate equal to 2kHz.These duties include going through the PMSM state machine, calibrating ADC current conversions, executing the speed controller, computing the new values of $I_{q,d_{\text{ref}}}$ for the FOC, and generating the PWM.

B. The safety loop Task

This task performs safety checks, for instance bus voltage and temperature, for all drive instance.The safety task starts by performing the average temperature as well as the over-current occurrence acquisition then proceeds to the voltage bus ADC conversion and to update the average value after that it performs faults processing and updates the state machine accordingly.If there is a fault, then the PWM generation is switched off, thus inactivating the outputs. The safety task ends with re-initializing the current and voltage variables in addition to clearing Park currents PI controllers, voltage sensor and Speed controller.

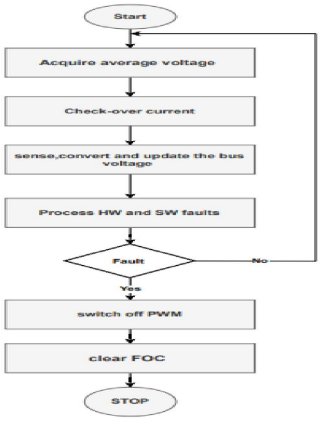

Fig. 4. The safety task flowchart

IV. Implementing and Explaining Diagnosis Tasks in STM32 PMSM Control Firmware:A Guide within a freeRTOS-Based Framework

Nowadays, motor diagnosis presents one of the most trendy goals, especially in the world, for the industry and E-Bike manufacturers. A better experience for the rider or the customer can be achieved by having smooth motor control. On the other hand, it will help to have safe driving and guarantee the user's safety. Multiple authors worked on the different types of faults present in E-bike system in the motor level. But the motor faults are treated separately and where the diagnosis suggested solutions are hard to put into an embedded target. The proposed solution for the e-bike's motor is to provide a complete diagnostic solution that is simpler to implement. The proposed freeRTOS-based PMSM firmware incorporates four tasks that address the critical diagnostic aspects. The importance of the diagnostic functionality lies in the dynamic variables we work with, namely, current, volt age, power, phase, and rotor position, and the need for the real-time monitoring of these variables which is paramount to the control of PMSM in e-bikes.
These four tasks execute the following functionalities: the HALL sensors diagnosis task, the power calculation task, the SOGI task, and the RMS calculation task.

A. The Hall sensors diagnosis task

The PMS motor with position sensor are mainly preferred, due to the limitations in sensorless applications, especially in the startup phase of the command and the speed range [13] The Hall sensors are likely preferred because of their simplicity and low cost [13].

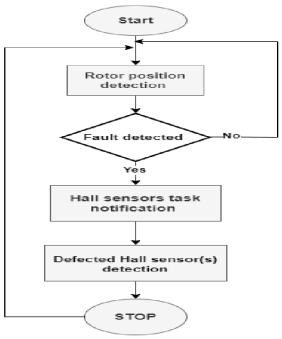

Fig. 5. The Hall sensors diagnosis task flowchart

The Hall sensors may be defected due to several causes including a harsh environment, violent vibration, faulty connection. In case of default presence, the defected Hall sensor might detect and reflect the real rotor position of the motor. This will lead to significant reduction in the dynamic performance of the motor or even overcurrent, which may cause extensive damage in the whole system [13]. The diagnosis task is created with a normal priority. Once created, this task enters the waiting state, unless a notification from the ISR is received.The diagnosis process is performed between the interrupt method of the Hall class that implements a motor control interrupt request function to be called when the position of the rotor is updated. Whenever a fault is detected in the interrupt request a task notification is performed through a task handler consequently giving the control to the diagnosis task where the processing of the diagnosis is performed. The implemented diagnosis solution, ensures the detection of double and single Hall sensor failure. The initial detection of the defect and the stopping of the motor is essentially related to the change a flag undergoes. Once this flag is false, the motor stops.

B. Open-phase Diagnosis

The open phase failure for the PMSM is commonly related to the disconnection of the phase winding from the power source as well an insulation problem in one of the inverter power switcher's legs. Although, it may be caused by other types of failure, including stator winding and mechanical failure of the terminal connector. The open phase fault may cause severe electromagnetic torque ripples and mechanical vibration. This deficiency leads to electromagnetic asymmetry on the stator and rotor. In either cases,the faulty phase

has a current value equal to zero [4]. Since the PMSM is known as a well-balanced load, the currents in the two other opposite-phase signals and their amplitude, increase by a factor of$\sqrt{3}$[4].

a) The SOGI task

The Second Order Generalized Integrator is used primarily to provide accurate estimation and tracking of the frequency and phase of the phase currents[7]. The power and energy applications widely recognize it as a prominent tool utilized for filtering and synchronization purposes. It finds practical application in diagnosing electric bikes by monitoring and analyzing the currents phase and amplitude, playing consequently the role of an embedded software sensor[8]. The Schematic Bloc 6 illustrates the SOGI algorithm.

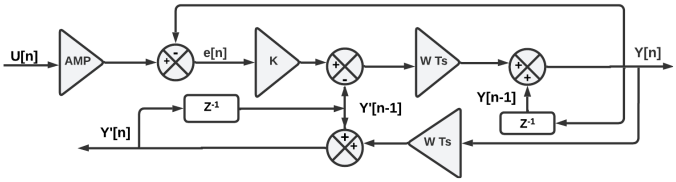

Fig. 6. General SOGI schematic bloc

The equations that describe the flow diagrams of the variables are to be set in the order that illustrates first the input variables and save the results to internal data as in equation1, and then we become able of arranging the set of equations for output variables in the correct Sequence allowing consequently the use of multi-step calculation of outputs. [8]

$$e_n = U_n - Y_n \tag{1}$$

$$Y_n = (K \cdot e_n - Y'_n) \cdot T_s \cdot W + Y_{n-1} \tag{2}$$

$$Y'_n = Y_{n-1} + T_s \cdot W \cdot Y_n \tag{3}$$

The equations show that we face the challenge of fixing the two parameters: the integration period T_s and the gain K in a way that guarantees the correct functioning of the SOGI. In this part of work,it is essential to respect the compromise between the SOGI and the system frequency interrupt. Since the input signal in our case directly depends on the ADC interrupt, we opted to use, the ISR frequency as T_s for the SOGI.

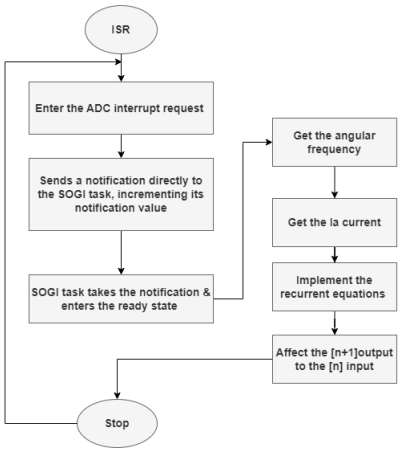

Fig. 7. SOGI task flowchart

b) RMS calculation task

Figure8 represents second open-phase solution detection.Where we opt for calculating RMS values in the context of diagnosing an e-bike because it allows us to monitor, track and assess the three phases' currents amplitudes. It actually does the same work as the SOGI task. The difference lays within the complexity of the task, as the SOGI task is based on linear recurrent equations whereas the RMS task relies on quadratic calculation as shown in the equation 4.With N : the length of the sliding window to get the average of the previous samples.

$$\mathbf{RMS} = \sqrt{\frac{1}{N}\sum_{n=0}^{N-1} x[n]^2} \tag{4}$$

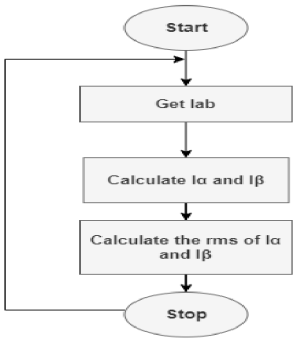

Fig. 8. RMS calculation task flowchart

C. Power-monitoring task

The power calculation task is part of the diagnosis tasks context. Since the e-bike depends on the battery as a finite source of energy, calculating the phase power and the average power becomes a crucial step towards achieving energy optimization and enables us to assess the performance of the e-bike by measuring the power consumption during different operating conditions, such as acceleration, climbing hills, or maintaining a constant speed, we can evaluate the efficiency and overall performance of the motor.

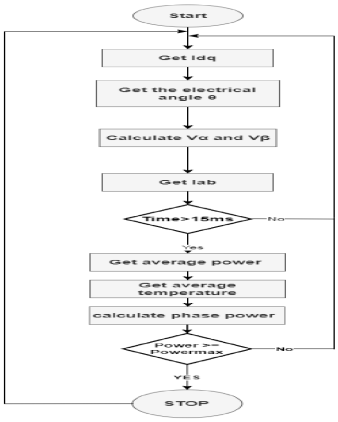

Fig. 9. Power calculation task flowchart

As evident from the flowchart in Fig.9, a deliberate choice has been made to introduce a 15ms waiting period before embarking on the calculation of phase powers or engaging

in the assessment of potential overpower conditions. This strategic pause is intended to facilitate the transition from the transient motor regime to a state of stable equilibrium within its permanent operational domain.

V. Experimental setup

The experimental setup shown in Fig.10 is composed of a 250W PMSM, a power supply delivering a Vdc=36V that emulates the role of a battery in e-bikes, an EVSPIN32G4 board, and the STM 32 cube IDE ensuring the upload of the program and the communication with the board via the motor pilot provided by ST. The Table 1 represents the different parameters of the used motor and the implemented SOGI

Fig. 10. Test setup

TABLE I
Experimental setup parameters

Parameter	Value
Motor Parameters	
Number of pole pairs	10
Maximum speed	1180 rpm
Nominal current	10 A
Nominal DC voltage	36 V
Stator resistance Rs	100 mΩ
Stator inductance Ls	0.19 mH
Nominal Power	250 W
Nominal torque	50 N/m
SOGI Parameters	
Integration period	10 μ s
Gain	2

A. Hall diagnosis results

A deformation in the plotting angle occurs when the hall sensor fault affects the measured feedback angle of the motor, as shown by the11. This will lead to a deformation in the speed dynamic, and the motor will no longer be able to follow the reference speed as shown in figure 12.

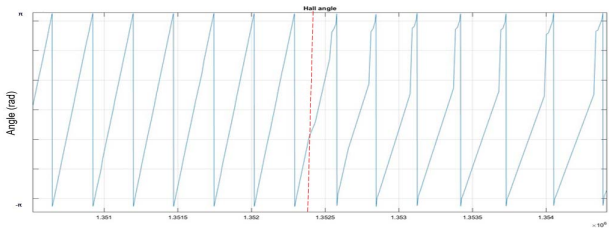

Fig. 11. Hall angles before and after a fault occurs

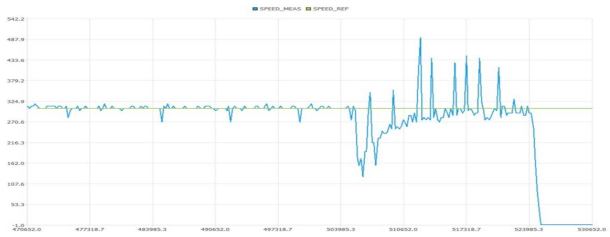

Fig. 12. Speed dynamic

After implementing the Hall sensor diagnosis module, the system became capable of detecting faulty hall sensors. The figures13 and 14represent the results of the firmware in both fault cases. During the first test, we only applied a single error to the Hall sensor, but in the second test, we encountered a double error.

Expression	Type	Value
start	uint32_t	0
fh1	_Bool	true
ps5	uint8_t [5]	[5]
HALL_M1	HALL_Handle_t	{...}
fh2	_Bool	false
fh3	_Bool	false
fh12	_Bool	false
fh23	_Bool	false
fh13	_Bool	false
count=count+1	uint32_t	2
count	uint32_t	1493
start_count	uint16_t	1

Fig. 13. Speed dynamic

Expression	Type	Value
start	uint32_t	0
fh1	_Bool	false
ps5	uint8_t [5]	[5]
HALL_M1	HALL_Handle_t	{...}
fh2	_Bool	false
fh3	_Bool	false
fh12	_Bool	true
fh23	_Bool	false
fh13	_Bool	false
count=count+1	uint32_t	2
count	uint32_t	768
start_count	uint16_t	1

Fig. 14. Speed dynamic

B. Open-Phase diagnosis results

In order to validate the operational efficacy of the freeRTOS-based PMSM control firmware, we harnessed the capabilities of the STM32Cube Monitor, to visualize in real time the motor control and diagnosis-related variables. Paramount among these variables were the currents, I_{ab}, I_d and I_q, alongside, the speed.Also,to validate the SOGI task experimentally,we visualized I_α and I_β .

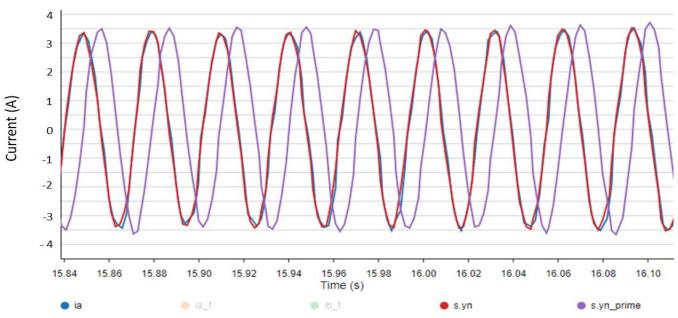

Fig. 15. Orthogonal voltage generator system y_n and y_{nprime}

The figure 15 illustrates i_α in-phase current, and the i_β quadrature-phase current. The in-phase signal is synchronized with the phase current i_a.

the Three-phase currents i_{abc} are balanced, it signifies a state of harmonious operation where the motor is functioning optimally. In this configuration, the currents flowing through each phase exhibit synchronized behavior, contributing to the motor's efficient performance.It is worth mentioning that we can only visualize ia and ib asic is deduced through the relation

$$ia + ib + ic = 0 \tag{5}$$

It shows, as well, i_a reaches a value of $3.5A$. This value is obtained as a result of amplifying the input U[n] that is equivalent to the phase current i_a by a gain equal to 10, as seen from the schematic block 6, to increase the error and visualize the output signals, since as we can see from the figure 16 the maximum value the currents reach is 0.35 A

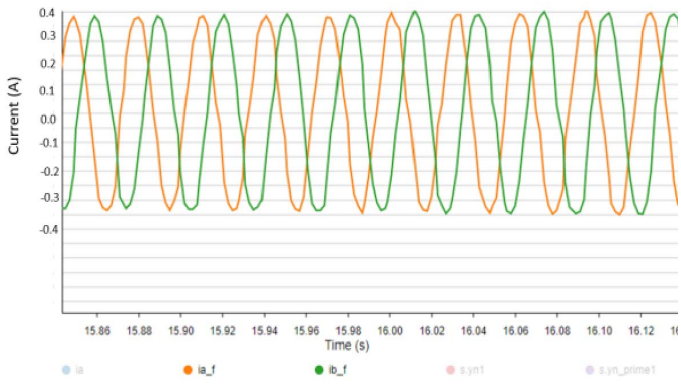

Fig. 16. ia and i_b phase current

VI. Conclusion

Nowadays, we face the challenge of achieving optimal control and diagnosis for e-bikes. In the scope of this challenge,this work has comprehensively unveiled the field-oriented control technique, elucidating its fundamental functional blocks. Additionally, this paper undertakes a comprehensive exploration of the STM32 freeRTOS-based firmware, incorporating both medium-frequency and safety tasks. These elements were expounded upon, explaining their structural frameworks through flowcharts along the execution processes underlying their functionalities. Furthermore, an approach was adopted to develop and implement the diagnosis tasks, notably the deferred interrupt handling and task notification mechanisms allowing seamless integration of diagnosis functions such as the hall sensors diagnosis task, the SOGI task, the power task, and the RMS calculation task. The experimental validation proves the reliability and efficiency of the control and diagnosis freeRTOS-based firmware, thus ensuring the optimal functioning of the e-bike. Through this holistic study, this work not only advances our understanding of STM32 freeRTOS -based motor control firmware but also offers a valuable reference for implementing robust and efficient control and diagnostic systems in e-bike applications.

Acknowledgment

The authors would like to express their gratitude to Actia Engineering Services Tunisia for the financial support of this research project.

References

[1] Korkmaz, Fatih et al. "Comparative performance evaluation of FOC and DTC controlled PMSM drives." In *4th International Conference on Power Engineering, Energy and Electrical Drives*, 2013, pp. 705–708. doi: 10.1109/PowerEng.2013.6635696.

[2] Hadla, Hazem and Santos, Fernando. "Performance Comparison of Field-oriented Control, Direct Torque Control, and Model-predictive Control for SynRMs." *Chinese Journal of Electrical Engineering* 8.1 (2022): 24–37. doi: 10.23919/CJEE.2022.000003.

[3] Richard Barry, *Mastering the FreeRTOS™ Real Time Kernel*, Version 161204, www.FreeRTOS.org

[4] Sejir Khojet El Khil, Imed Jlassi, Antonio J. Marques Cardoso, Jorge O. Estima, and Najiba Mrabet-Bellaaj, "Diagnosis of open-switch and current sensor faults in PMSM drives through stator current analysis," *IEEE Transactions on Industry Applications*, vol. 55, no. 6, pp. 5925–5937, 2019.

[5] Li, P. et al. "Design of motor control driver based on arm and freertos." In *CSAA/IET International Conference on Aircraft Utility Systems (AUS 2020)*, 2020, pp. 897–902. doi: 10.1049/icp.2021.0363.

[6] NXP semiconductors. *Motor Control Using FreeRTOS*, 2020. (AN12881 Rev. 0 — May, 2020)

[7] Ahlem Ben Youssef, Sejir Khojet El Khil, and Ilhem Slama-Belkhodja, "State observer-based sensor fault detection and isolation, and fault tolerant control of a single-phase PWM rectifier for electric railway traction," *IEEE Transactions on Power Electronics*, vol. 28, no. 12, pp. 5842–5853, 2013.

[8] Rafal, Krzysztof et al. "Application of the second order generalized integrator in digital control systems." *Archives of Electrical Engineering* 63 (2014): 2014. doi: 10.2478/aee-2014-0031.

[9] Wang, Gaolin, et al. "Rotor position estimation of PMSM in low-speed region and standstill using zero-voltage vector injection." *IEEE Transactions on Power Electronics* 33.9 (2017): 7948-7958.

[10] Lee, Jin-Shyan, Jun-Wei Jiang, and Yuan-Heng Sun. "Design and simulation of control systems for electric-assist bikes." *2016 IEEE 11th Conference on Industrial Electronics and Applications (ICIEA)* IEEE, 2016.

[11] Hung, Nguyen Ba, and Ocktaeck Lim. "A review of history, development, design and research of electric bicycles." *Applied Energy* 260 (2020): 114323.

[12] Contò, Chiara, and Nicola Bianchi. "E-Bike Motor Drive: A Review of Configurations and Capabilities." *Energies 16.1* (2022): 160.

[13] Zhang, Xi, et al. "Real-time fault diagnosis and fault-tolerant control strategy for Hall sensors in permanent magnet brushless DC motor drives." *Electronics10.11* (2021): 1268.